Novel Phosphorescent Cyclometalated Organotin(IV) and Organolead(IV) Complexes of 2,6-Bis(2′-indolyl)pyridine and 2,6-Bis[2′-(7-azaindolyl)]pyridine

Wen-Li Jia, Qin-De Liu, Ruiyao Wang, and Suning Wang*

Department of Chemistry, Queen's University, Kingston, Ontario K7L 3N6, Canada

Received May 29, 2003

Four novel five-coordinated Sn(IV) and Pb(IV) complexes of 2,6-bis(2′-indolyl)pyridine (H_2-bip) and 2,6-bis[2′-(7-azaindolyl)]pyridine (H_2bap) were synthesized. These four complexes have the formulas Sn(bip)Ph_2 (**1**), Sn(bap)Ph_2 (**2**), Pb(bip)Ph_2 (**3**), and Pb(bap)Ph_2 (**4**), respectively. The structures were determined by single-crystal X-ray diffraction. In the complexes, the metal centers are tridentately chelated by the bip or the bap ligand and further coordinated by two phenyl groups, resulting in a distorted-trigonal-bipyramidal geometry. These complexes display interesting extended $\pi-\pi$ stack structures in the solid state. Complexes **1** and **2** are luminescent at room temperature in solution and the solid state. At 77 K in THF solution, all four complexes display both blue-green fluorescent and orange-red phosphorescent emissions, which originate from ligand-centered $\pi \rightarrow \pi^*$ transitions. The Sn(IV) and Pb(IV) centers play a key role in enhancing phosphorescent emission of the bip and bap ligands.

Introduction

Luminescent organic/organometallic compounds have attracted much attention recently due to their potential applications in sensor technologies and photochemical and electroluminescent devices.[1−3] In comparison with fluorescent compounds, phosphorescent compounds are more attractive for applications in organic light-emitting devices (OLEDs) because of their potential in the enhancement of the overall device efficiency.[4] However, the emissions of most luminescent organic compounds are dominated by fluorescence, and their phosphorescent emissions are either negligible or very weak. To promote the phosphorescent emissions, heavy-metal centers are often introduced into the organic ligands, as it has been demonstrated that metal centers can play a key role in promoting singlet−triplet state mixing and, hence, phosphorescent emission.[4] Many recent studies on phosphorescent compounds concern metal complexes involving d-block metal centers such as Pt(II) and Ir(III).[4,5] Due to the presence of the incomplete 5d shell, these transition-metal ions very often quench the emission from the ligand, although phosphorescence due to MLCT transitions has been observed frequently. Among the phosphorescent organometallic compounds, cyclometalated complexes are the most attractive, due to their high stability and rigidity that reduces the loss of energy by thermal vibrational decay.[6] Since heavy main-group metals, such as lead and bismuth, also display strong spin−orbital coupling, they could play the same role as heavy transition-metal atoms in promoting phosphorescent emission. Furthermore, $(n - 1)$d electrons in the main-group metal centers usually do not interfere with the electronic transitions of the ligand

(1) (a) Tang, C. W.; VanSlyke, S. A. *Appl. Phys. Lett.* **1987**, *51*, 913. (b) Tang, C. W.; VanSlyke, S. A.; Chen, C. H. *J. Appl. Phys.* **1989**, *65*, 3610. (c) Hu, N.-X.; Esteghamatian, M.; Xie, S.; Popovic, Z.; Ong, B.; Hor, A. M.; Wang, S. *Adv. Mater.* **1999**, *11*, 1460. (d) Bulovic, V.; Gu, G.; Burrows, P. E.; Forrest, S. R.; Thompson, M. E. *Nature* **1996**, *380*, 29. (e) Balzani, V.; Juris, A.; Venturi, M.; Campagna, S.; Serroni, S. *Chem. Rev.* **1996**, *96*, 759. (f) Shen, Z.; Burrows, P. E.; Bulovic, V.; Forrest, S. R.; Thompson, M. E. *Science* **1997**, *276*, 2009. (g) Paplovski, D. B. *Sens. Actuators, B* **1995**, *29*, 213. (h) Ma. Y.; Che, C.-M.; Chao, H.-Y.; Zhou, X.; Chan, W.-H.; Shen, *J. Adv. Mater.* **1999**, *11*, 852. (i) Poterini, G.; Serpone, N.; Bergkamp, M. A.; Netzel, T. L. *J. Am. Chem. Soc.* **1983**, *105*, 4639. (j) Papkovski, D. B.; Ponomarev, G. V.; Kurochkin, I. N.; Korpela, T. *Anal. Lett.* **1995**, *28*, 2027.

(2) (a) Adachi, A.; Baldo, M. A.; Forrest, S. R.; Lamansky, S.; Thompson, M. E.; Kwong, R. C. *Appl. Phys. Lett.* **2001**, *78*, 1622. (b) Adachi, A.; Kwong, R. C.; Djurovich, P.; Adamovich, V.; Baldo, M. A.; Thompson, M. E.; Forrest, S. R. *Appl. Phys. Lett.* **2001**, *79*, 2082. (c) O'Brien, D. F.; Baldo, M. A.; Lamansky, S.; Burraw, P. E.; Thompson, M. E.; Forrest, S. R. *Appl. Phys. Lett.* **1999**, *75*, 4. (d) Sprouse, S.; King, K. A.; Spellane, P. J.; Watts, R. J. *J. Am. Chem. Soc.* **1984**, *106*, 6647.

(3) (a) Wu, Q.; Esteghamatian, M.; Hu, N.-X.; Popovic, Z.; Enright, G.; Tao, Y.; D'Iorio, M.; Wang, S. *Chem. Mater.* **2000**, *12*, 79. (b) Wu, Q.; Esteghamatian M.; Hu, N.-X.; Popovic, Z.; Enright, G.; Breeze, S. R.; Wang, S. *Angew. Chem., Int. Ed.* **1999**, *38*, 985. (c) Pang J.; Tao Y.; Freiberg. S.; Yang, X. P.; D'Iorio, M.; Wang, S. *J. Mater. Chem.* **2002**, *12*, 206. (d) Pang, J.; Marotte, E. J. P.; Seward, C.; Brown, R. S.; Wang, S. *Angew. Chem., Int. Ed.* **2001**, *40*, 4042.

(4) (a) Baldo, M. A.; Thompson, M. E.; Forrest, S. R. *Nature* **2000**, *403*, 750. (b) Kwong, R. C.; Sibley, S.; Dubovoy, T.; Baldo, M. A.; Forrest, S. R.; Thompson, M. E. *Chem. Mater.* **1999**, *11*, 3709. (c) Kwong, R. C.; Lamansky, S.; Thompson, M. E. *Adv. Mater.* **2000**, *12*, 1134. (d) Lamansky, S.; Djurovich, P.; Murphy, D.; Abdel-Razzag, F.; Lee, H.-E.; Aadachi, C.; Burrows, P. E.; Forrest, S. R.; Thompson, M. E. *J. Am. Chem. Soc.* **2001**, *123*, 4304. (e) Lamansky, S.; Djurovich, P.; Murphy, D.; Abdel-Razzag, F.; Kwong, R. C.; Tsyba, I.; Bortz, M.; Mui, B.; Bau, R.; Thompson, M. E. *Inorg. Chem.* **2001**, *40*, 1704.

(5) (a) Pomestchenko, I. E.; Luman, C. R.; Hissler, M.; Ziessel, R.; Castellano, F. N. *Inorg. Chem.* **2003**, *42*, 1394. (b) Brooks, J.; Babayan, Y.; Lamansky, S.; Djurovich, P.; Tsyba, I.; Bau, R.; Thompson, M. E. *Inorg. Chem.* **2002**, *41*, 3055. (c) Duan, J. P.; Sun, P. P.; Chen, C. H. *Adv. Mater.* **2003**, *15*, 224. (d) Chen, F. C.; He, C. F.; Yang, Y. *Appl. Phys. Lett.* **2003**, *82*, 1006. (e) Adachi, C.; Baldo, M. A.; Thompson, M. E.; Forrest, S. R. *J. Appl. Phys.* **2001**, *90*, 5048.

(6) (a) Lakowicz, J. R. *Principles of Fluorescence Spectroscopy*, 2nd ed.; Kluwer Academic: New York, 1999. (b) Ingle, J. D.; Crouch, S. R., Jr. *Spectrochemical Analysis*; Prentice Hall: Englewood Cliffs, NJ, 1988; Chapter 12.

10.1021/om030404a CCC: $25.00
Publication on Web 08/28/2003

Chart 1

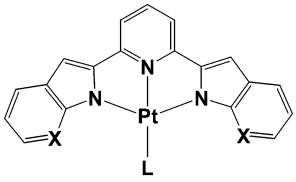

L = Py, SMe_2

because of their closed shell. On the other hand, the availability of the unoccupied *n*d orbitals of the heavy main-group elements allows valence expansion and the accommodation of multidentate ligands. Despite the potential of main-group phosphorescent compounds, reports concerning phosphorescent emission promoted by main-group-metal centers are surprisingly scarce. We have reported a number of phosphorescent group 15 compounds recently that contain terminal aryl ligands functionalized by 7-azaindolyl or 2,2′-dipyridylamino groups, where the heavier group 15 elements were shown to drastically enhance phosphorescent emission of the ligands.[7] Although many luminescent cyclometalated complexes with d-block metals have been reported,[8] phosphorescent cyclometalated main-group compounds are rare. The heavy elements of group 14 at oxidation state +4 are known to display versatile coordination numbers and geometries and, hence, may be suitable for the formation of cyclometalated compounds. To our knowledge, no phosphorescent Pb(IV) or Sn(IV) cyclometalated complexes have been reported before. Our investigation therefore focused on cyclometalated Sn(IV) and Pb(IV) compounds. This investigation is based on the results of our recent work on several cycloplatinated complexes with 2,6-bis(2′-indolyl)pyridine (H_2bip), Pt(bip)L, which emit bright orange-red phosphorescence originating from ligand-centered $\pi \rightarrow \pi^*$ transitions (Chart 1) and were demonstrated to be useful emitters in OLEDs.[9] Our work on the Pt(II) bip complexes indicated that the bip ligand is potentially useful for the emission of phosphorescence in the presence of a metal ion. Herein we report the results of our investigation on using the H_2bip ligand and the related 2,6-bis[2′-(7-azaindolyl)]pyridine (H_2bap) ligand to form phosphorescent cyclometalated Sn(IV) and Pb(IV) complexes.

Experimental Section

All starting materials were analytical reagents purchased from Aldrich Chemical Co. and were used without further purification. All solvent used in syntheses and spectroscopic measurements were distilled over appropriate drying reagents. ^{1}H, ^{13}C, and ^{119}Sn NMR spectra were recorded on a Bruker Advance 500 spectrometer operating at 500 MHz for ^{1}H, 125.7 MHz for ^{13}C, and 186.4 MHz for ^{119}Sn, respectively. Excitation and emission spectra were obtained with a Photon Technologies International QuantaMaster Model C-60 spectrometer. Emission lifetime was measured on a Photon Technologies International Phosphorescent lifetime spectrometer, Timemaster C-631F, equipped with a xenon flash lamp and digital emission photon multiplier tube using a band pathway of 5 nm for excitation and 2 nm for emission. UV−vis spectra were recorded on a Hewlett-Packard 8562A diode array spectrophotometer. Elemental analyses were performed by Canadian Microanalytical Service Ltd., Delta, British Columbia, Canada. The free ligand[10] 2,6-bis(2′-indolyl)pyridine and $PbCl_2Ph_2$ were prepared using a previously reported procedure.[11]

Synthesis of 2,6-Bis[1′-(phenylsulfonyl)-2′-(7′-azaindolyl)]pyridine. To a solution of *N*-(phenylsulfonyl)-7-azaindole (5.835 g, 22.5 mmol) in 40 mL of THF at 0 °C was slowly added a solution of LDA (1.5 M in cyclohexane, 16.6 mL, 24.9 mmol). The resulting mixture was stirred for 30 min at this temperature, and then a solution of $ZnCl_2$ (0.5M in THF, 49.8 mL, 24.9 mmol) was added. The mixture was stirred at room temperature for another 30 min. In a separate flask a solution of 2,6-dibromopyridine (2.06 g, 9.69 mmol) in 15 mL of THF was added to a solution containing a catalyst prepared by the reaction of $Pd(PPh_3)_2Cl_2$ (0.489 g, 0.696 mmol) in 10 mL of THF with diisobutylaluminum hydride (1.0 M in hexane, 1.39 mL, 1.39 mmol), and the mixture was stirred for 20 min at room temperature. The resulting mixture was refluxed for 6 h, cooled to room temperature, and poured into saturated aqueous Na_2CO_3. The aqueous phase was extracted with Et_2O, and the organic extracts were concentrated to give a brown residue, which was purified by column chromatography (hexane/CH_3CO_2Et, 6/1) to obtain the product in 57% yield. ^{1}H NMR ($CDCl_3$; δ, ppm): 8.60 (dd, 2H, J = 4.8, 1.5 Hz), 7.95−8.00 (m, 7H), 7.77 (d, 2H, J = 7.8 Hz), 7.32 (dd, 2H, J = 7.8, 1.8 Hz), 7.07 (t, 2H, J = 7.5 Hz), 6.91 (s, 2H), 6.68 (dd, 4H, J = 8.4, 1.5 Hz).

Synthesis of 2,6-Bis[2′-(7′-azaindolyl)]pyridine (H_2bap). A mixture of 2,6-bis[1′-(phenylsulfonyl)-2′-(7′-azaindolyl)]pyridine (1.92 g, 3.25 mmol) in EtOH (320 mL) and 10% aqueous NaOH (30 mL) was heated at reflux overnight. The resulting mixture was concentrated, and the residue was dissolved in CH_2Cl_2. The solution was washed with water and aqueous Na_2CO_3, dried, and concentrated. Column chromatography (THF/hexane, 1/1) of the residue afforded a yellow compound in 90% yield. ^{1}H NMR (DMSO-d_6; δ, ppm): 8.33 (d, 2H, J = 4.4 Hz), 8.04 (d, 2H, J = 7.8 Hz), 8.00 (d, 2H, J = 7.0 Hz), 7.94 (t, 1H, J = 6.6 Hz), 7.29 (s, 2H), 7.13 (dd, 2H, J = 7.8, 4.6 Hz). ^{13}C NMR (DMSO-d_6; δ, ppm): 150.0, 145.0, 138.8, 138.2, 129.8, 125.8, 121.8, 119.4, 117.1, 100.0.

Sn(bip)Ph_2 (1). Under N_2 protection, 2,6-bis(2′-indolyl)pyridine (H_2bip, 150 mg, 0.48 mmol) was dissolved in 10 mL of Na that was pretreated and freshly distilled from THF. The solution was cooled to −78 °C with dry ice/acetone. Then 0.64 mL of 1.6 M butyllithium solution (1.02 mmol) in hexane was added slowly. After the mixture was stirred for 40 min at −78 °C, 10 mL of a THF solution containing 171 mg (0.50 mmol) of $SnCl_2Ph_2$ was added. The solution was stirred for 40 min at −78 °C and warmed to ambient temperature. The reaction mixture was stirred for another 2 h, the solvent was removed under vacuum, and the residue was dissolved in 10 mL of CH_2Cl_2. After the white insoluble solid (LiCl) was removed by filtration, anhydrous toluene (5 mL) was layered upon the

(7) Kang, Y.; Song, D.; Schmider, H.; Wang, S. *Organometallics* **2002**, *21*, 2413.

(8) (a) McMillin, D. R.; Moore, J. J. *Coord. Chem. Rev.* **2002**, *229*, 113 and references therein. (b) Field, J. S.; Haines, R. J.; McMillin, D. R.; Summerton, G. C. *J. Chem. Soc., Dalton Trans.* **2002**, 1369. (c) Moore, J. J.; Nash, J. J.; Fanwick, P. E.; McMillin, D. R. *Inorg. Chem.* **2002**, *41*, 6387. (d) Yutaka, T.; Mori, I.; Kurihara, M.; Mizutani, J.; Tamai, N.; Kawai, T.; Irie, M.; Nishihara, H. *Inorg. Chem.* **2002**, *41*, 7143. (e) Yang, Q. Z.; Wu, L. Z.; Wu, Z. X.; Zhang, L. P.; Tung, C. H. *Inorg. Chem.* **2002**, *41*, 5653. (f) Yam, V. W. W.; Wong, K. M. C.; Zhu, N. *J. Am. Chem. Soc.* **2002**, *124*, 6506. (g) Yam, V. W. W.; Hui, C. K.; Wong, K. M. C.; Zhu, N.; Cheung, K. K. *Organometallics* **2002**, *21*, 4326. (h) Che, C. M.; Zhang, J. L.; Lin, L. R. *Chem. Commun.* **2002**, 2556. (i) Che, C. M.; Fu, W. F.; Lai, S. W.; Hou, Y. J.; Liu, Y. L. *Chem. Commun.* **2003**, 118. (j) Lu, W.; Zhu, N.; Che, C. M. *Chem. Commun.* **2002**, 900. (k) Hui, C. K.; Chu, B. W. K.; Zhu, N.; Yam, V. W. W. *Inorg. Chem.* **2002**, *41*, 6178. (l) Lamansky, S.; Djurovich, P. I.; Abdel-Razzq, F.; Garon, S.; Murphy, D. L.; Thompson, M. E. *J. Appl. Phys.* **2002**, *92*, 1570.

(9) Liu, Q. D.; Thorne, L.; Kozin, I.; Song, D.; Seward. C.; D'Iorio, M.; Tao, Y.; Wang, S. *J. Chem. Soc., Dalton Trans.* **2002**, 3234.

(10) Thummel, R. P.; Hegde, V. *J. Org. Chem.* **1989**, *54*, 1720.

(11) Gilman, H.; Robinson, J. D. *J. Am. Chem. Soc.* **1929**, *51*, 3112.

Table 1. Crystal Data

	1	2	3	4
formula	$C_{33}H_{23}N_3Sn{\cdot}C_7H_8$	$C_{31}H_{21}N_5Sn{\cdot}CH_2Cl_2$	$C_{33}H_{23}N_3Pb{\cdot}CH_2Cl_2$	$C_{31}H_{21}N_5Pb{\cdot}0.5H_2O$
fw	672.37	667.14	753.66	679.73
cryst syst	triclinic	triclinic	triclinic	triclinic
space group	$P\bar{1}$	$P\bar{1}$	$P\bar{1}$	$P\bar{1}$
a/Å	9.480(3)	11.304(16)	11.969(2)	11.894(3)
b/Å	12.952(4)	11.507(17)	13.740(3)	13.443(3)
c/Å	14.564(5)	13.823(18)	19.676(3)	17.985(5)
α/deg	66.301(5)	69.03(2)	79.344(4)	94.283(6)
β/deg	76.902(5)	69.25(2)	85.782(4)	92.072(5)
γ/deg	79.502(5)	60.587(19)	67.230(4)	114.293(5)
V/Å^3	1586.6(9)	1427(3)	2932.2(9)	2606.6(11)
Z	2	2	4	4
D_c/g cm^{-3}	1.407	1.553	1.707	1.732
μ/mm^{-1}	0.838	1.114	5.964	6.504
$2\theta_{max}$/deg	56.60	56.76	56.66	56.62
no. of rflns measd	11 545	10 513	21 247	18 699
no. of rflns used (R_{int})	7327 (0.0248)	6635 (0.0557)	13 458 (0.0145)	11 912 (0.0548)
no. of params	378	367	721	676
final R ($I > 2\sigma(I)$)				
R1[a]	0.0563	0.0555	0.0292	0.0582
wR2[b]	0.1483	0.0893	0.0581	0.0776
R (all data)				
R1[a]	0.0902	0.1824	0.0532	0.2010
wR2[b]	0.1603	0.1077	0.0616	0.1003
goodness of fit on F^2	0.936	0.696	0.871	0.768

[a] $R1 = \sum[|F_o| - |F_c|]/\sum|F_o|$. [b] $wR2 = \{\sum[w(F_o^2 - F_c^2)]/\sum(wF_o^2)\}^{1/2}$, $w = 1/[\sigma^2(F_o^2) + (0.075P)^2]$, $P = [\mathrm{Max}(F_o^2,0) + 2F_c^2]/3$.

filtrate. The two-layered solution was then allowed to stand at ambient temperature. Slow diffusion and evaporation of the solvent afforded **1** as orange crystals, which lost crystal lattice solvent quickly and became a yellow powder after several days (188 mg, 68% yield). ^{1}H NMR (CD_2Cl_2; δ, ppm): 7.98 (t, 1H, J = 7.4 Hz, Py), 7.75−7.78 (m, 4H, Py and indolyl), 7.70 (dd, 4H, J = 7.8, 1.7 Hz, Ph), 7.47 (dd, 2H, J = 8.2, 0.8 Hz, indolyl), 7.30−7.37 (m, 8H, Ph and indolyl), 7.20 (ddd, 2H, J = 8.2, 6.9, 1.3 Hz, indolyl), 7.10 (ddd, 2H, J = 8.0, 7.0, 1.0 Hz, indolyl). ^{13}C NMR (CD_2Cl_2; δ, ppm): 149.8, 145.2, 143.0, 140.2, 137.6, 136.5 (with satellites, J_{Sn-C} = 61.9 Hz), 133.7, 131.9, 129.7 (with satellites, J_{Sn-C} = 83.9 Hz), 124.2, 122.5, 120.2, 117.3, 115.6, 103.6. ^{119}Sn NMR (CD_2Cl_2; δ, ppm, vs $SnMe_4$): −299.6. Anal. Calcd for $C_{33}H_{23}N_3Sn$: C, 68.30; H, 4.00; N, 7.25. Found: C, 68.44; H, 4.17; N, 7.12.

Sn(bap)Ph$_2$ (2). This complex was obtained in the same manner as that described for **1**, except using hexane instead of toluene. The reaction of H_2bap (150 mg, 0.48 mmol) and $SnCl_2Ph_2$ (171 mg, 0.50 mmol) provided **2** as yellow crystals (230 mg, 72% yield). ^{1}H NMR (CD_2Cl_2; δ, ppm): 8.49 (dd, 2H, J = 4.5, 2.0 Hz, 7-azaindolyl), 8.10 (dd, 2H, J = 7.5, 2.0 Hz, 7-azaindolyl), 8.05 (t, 1H, J = 8.0 Hz, Py), 8.01 (dd, 4H, J = 8.0, 1.5 Hz, Ph), 7.85 (d, 2H, J = 8.0 Hz, Py), 7.33 (tt, 2H, J = 7.5, 1.5 Hz, Ph), 7.30 (s, 2H, 7-azaindolyl), 7.26 (t, 4H, J = 7.5 Hz, Ph), 7.13 (dd, 2H, J = 8.0, 4.5 Hz, 7-azaindolyl). ^{13}C NMR (CD_2Cl_2; δ, ppm): 155.8, 149.6, 145.9, 142.8, 137.5, 137.1, 130.5, 129.9, 128.9, 125.0, 117.8, 116.3, 101.4 (one quaternary carbon hidden). ^{119}Sn NMR (CD_2Cl_2; δ, ppm, vs $SnMe_4$): −289.2. Anal. Calcd for $C_{33}H_{23}N_3Sn{\cdot}{}^1/_3CH_2Cl_2$: C, 61.60; H, 3.44; N, 11.47. Found: C, 61.69; H, 3.86; N, 11.87.

Pb(bip)Ph$_2$ (3). This complex was obtained in the same manner as that described for **1**. The reaction of H_2bip (100 mg, 0.32 mmol) and $PbCl_2Ph_2$ (140 mg, 0.32 mmol) provided **3** as orange crystals at first, which changed to dark red crystals after several days due to the replacement of crystal lattice molecules from CH_2Cl_2 to toluene (165 mg, 64% yield). ^{1}H NMR (CD_2Cl_2; δ, ppm): 7.92 (t, 1H, J = 8.0 Hz, Py), 7.82 (d, 2H, J = 8.0 Hz, indolyl), 7.79 (d, 2H, J = 8.0 Hz, Py), 7.77 (dd, 2H, J = 8.2, 0.8 Hz, indolyl), 7.74 (dd, 4H, J = 8.2, 1.3 Hz, Ph), 7.41 (t, 4H, J = 8.0 Hz, Ph), 7.35 (tt, 2H, J = 8.0, 1.3 Hz, Ph), 7.33 (s, 2H, indolyl), 7.30 (ddd, 2H, J = 8.1, 6.9, 1.2 Hz, indolyl), 7.14 (ddd, 2H, J = 7.9, 6.9, 0.8 Hz, indolyl). ^{13}C NMR (CD_2Cl_2; δ, ppm): 157.6, 151.2, 146.6, 141.2, 140.2, 135.4 (with satellites, J_{Pb-C} = 124.7 Hz), 133.0, 131.1 (with satellites, J_{Pb-C} = 169.1 Hz), 131.0, 123.4, 121.9, 119.4, 117.6, 114.8, 103.0. Anal. Calcd for $C_{33}H_{23}N_3Pb{\cdot}C_7H_8$: C, 63.14; H, 4.11; N, 5.52. Found: C, 62.70; H, 4.26; N, 5.39.

Pb(bap)Ph$_2$ (4). This complex was obtained in the same manner as that described for **2**. The reaction of H_2bap (100 mg, 0.32 mmol) and $PbCl_2Ph_2$ (140 mg, 0.32 mmol) provided **4** as orange crystals (135 mg, 63% yield). ^{1}H NMR (CD_2Cl_2; δ, ppm): 8.46 (dd, 2H, J = 4.6, 1.6 Hz, 7-azaindolyl), 8.14 (dd, 2H, J = 7.9, 1.6 Hz, 7-azaindolyl), 7.91−7.95 (m, 5H, Py and Ph), 7.83 (d, 2H, J = 7.7 Hz, Py), 7.36 (t, 4H, J = 7.6 Hz, Ph), 7.31 (tt, 2H, J = 7.4, 1.5 Hz, Ph), 7.23 (s, 2H, 7-azaindolyl), 7.11 (dd, 2H, J = 7.9, 4.6 Hz, 7-azaindolyl). ^{13}C NMR (CD_2Cl_2; δ, ppm): 159.3, 157.0, 151.2, 145.0, 141.0, 137.8, 135.4 (with satellites, J_{Pb-C} = 125.7 Hz), 130.7 (with satellites, J_{Pb-C} = 163.4 Hz), 129.4, 129.2, 124.8, 118.2, 115.5, 100.7. Anal. Calcd for $C_{33}H_{23}N_3Pb{\cdot}0.5H_2O$: C, 54.79; H, 3.24; N, 10.31. Found: C, 55.13; H, 3.32; N, 9.89.

X-ray Crystallographic Analysis. Single crystals of the free ligands H_2bip and H_2bap were obtained from slow evaporation of THF solutions. Crystals for **1** and **3** were obtained from slow diffusion of toluene into CH_2Cl_2 solutions, while crystals of **2** and **4** were obtained from slow diffusion of hexane into CH_2Cl_2 solutions. All crystals except that of **1** were mounted on glass fibers for data collection. Single crystals of **1** contain toluene solvent molecules and lose the solvent molecule rapidly. Therefore, the crystal of **1** was sealed in a thin-walled glass capillary for the structure determination. Data were collected on a Siemens P4 single-crystal X-ray diffractometer with a CCD-1000 detector and graphite-monochromated Mo Kα radiation, operating at 50 kV and 30 mA at 25 °C. Two different forms of single crystals of complex **3** were isolated and analyzed, one of which contains one CH_2Cl_2 per molecule of **3** and the other of which contains 1.5 toluene molecule per molecule of **3**. The data collection ranges over the 2θ ranges are 4.00−56.58° for H_2bip, 3.10−56.60° for H_2bap and **1**, 3.24−56.76° for **2**, 3.26−56.66° for **3**$\cdot CH_2Cl_2$, 3.04−56.64° for **3**$\cdot 1.5C_7H_8$, and 3.34−56.62° for **4**. No significant decay was observed for any sample. Data were processed on a PC using the Bruker SHELXTL software package[12] (version 5.10) and are corrected for Lorentz and polarization effects. The free ligands H_2bip and H_2bap crystallize in the

(12) SHELXTL NT Crystal Structure Analysis Package, version 5.10; Bruker AXS, Analytical X-ray System, Madison, WI, 1999.

Table 2. Selected Bond Lengths (Å) and Angles (deg) for Complexes 1−4

	Complex **1**		
Sn(1)−C(1)	2.123(5)	Sn(1)−C(7)	2.102(5)
Sn(1)−N(1)	2.163(4)	Sn(1)−N(2)	2.180(2)
Sn(1)−N(3)	2.162(5)		
N(1)−Sn(1)−N(2)	148.19(19)	N(1)−Sn(1)−N(3)	74.42(18)
N(1)−Sn(1)−C(1)	99.18(17)	N(1)−Sn(1)−C(7)	96.22(18)
N(2)−Sn(1)−N(3)	73.77(18)	N(2)−Sn(1)−C(1)	95.35(18)
N(2)−Sn(1)−C(7)	97.75(18)	N(3)−Sn(1)−C(1)	116.45(17)
N(3)−Sn(1)−C(7)	117.38(17)	C(1)−Sn(1)−C(7)	126.15(19)
	Complex **2**		
Sn(1)−C(1)	2.079(7)	Sn(1)−C(7)	2.121(6)
Sn(1)−N(1)	2.154(6)	Sn(1)−N(2)	2.176(6)
Sn(1)−N(3)	2.224(6)		
N(1)−Sn(1)−N(2)	145.9(2)	N(1)−Sn(1)−N(3)	72.6(2)
N(1)−Sn(1)−C(1)	99.7(3)	N(1)−Sn(1)−C(7)	94.8(3)
N(2)−Sn(1)−N(3)	73.3(2)	N(2)−Sn(1)−C(1)	96.5(3)
N(2)−Sn(1)−C(7)	98.3(3)	N(3)−Sn(1)−C(1)	115.5(2)
N(3)−Sn(1)−C(7)	115.9(2)	C(1)−Sn(1)−C(7)	128.6(2)
	Complex **3**·CH_2Cl_2		
Pb(1)−C(1)	2.161(4)	Pb(1)−C(7)	2.177(4)
Pb(1)−N(1)	2.296(3)	Pb(1)−N(2)	2.317(3)
Pb(1)−N(3)	2.295(3)		
N(1)−Pb(1)−N(2)	142.36(13)	N(1)−Pb(1)−N(3)	71.24(12)
N(1)−Pb(1)−C(1)	98.42(15)	N(1)−Pb(1)−C(7)	94.10(13)
N(2)−Pb(1)−N(3)	71.12(13)	N(2)−Pb(1)−C(1)	95.17(15)
N(2)−Pb(1)−C(7)	98.85(13)	N(3)−Pb(1)−C(1)	111.58(13)
N(3)−Pb(1)−C(7)	110.23(13)	C(1)−Pb(1)−C(7)	138.19(15)
	Complex **4**		
Pb(1)−C(1)	2.182(10)	Pb(1)−C(7)	2.175(10)
Pb(1)−N(1)	2.392(11)	Pb(1)−N(2)	2.366(9)
Pb(1)−N(3)	2.374(11)	Pb(2)−C(32)	2.136(12)
Pb(2)−C(38)	2.161(12)	Pb(2)−N(6)	2.335(9)
Pb(2)−N(7)	2.367(9)	Pb(2)−N(8)	2.340(10)
N(1)−Pb(1)−N(2)	138.3(5)	N(1)−Pb(1)−N(3)	70.5(5)
N(1)−Pb(1)−C(1)	93.1(4)	N(1)−Pb(1)−C(7)	91.1(4)
N(2)−Pb(1)−N(3)	68.0(4)	N(2)−Pb(1)−C(1)	98.2(4)
N(2)−Pb(1)−C(7)	95.6(4)	N(3)−Pb(1)−C(1)	100.5(3)
N(3)−Pb(1)−C(7)	105.0(4)	C(1)−Pb(1)−C(7)	154.0(4)
N(6)−Pb(2)−N(7)	138.5(5)	N(6)−Pb(2)−N(8)	69.3(4)
N(6)−Pb(2)−C(32)	95.8(4)	N(6)−Pb(2)−N(38)	99.8(4)
N(7)−Pb(2)−N(8)	69.2(5)	N(7)−Pb(2)−C(32)	92.8(4)
N(7)−Pb(2)−C(38)	94.1(4)	N(8)−Pb(2)−C(32)	101.1(4)
N(8)−Pb(2)−C(38)	111.2(4)	C(32)−Pb(2)−C(38)	147.4(5)

monoclinic space group $P2_1/c$, and the crystals of all the complexes belong to the triclinic space group $P\bar{1}$, but with unit cell parameters quite different from each other. All structures were solved by direct methods. One toluene per molecule of **1** was located in the crystal lattice of **1**. One CH_2Cl_2 molecule per molecule of **2** was located in the crystal lattice of **2**. Compound **4** contains 0.5 H_2O molecule per molecule of **4**. The free ligand H_2bip cocrystallizes with one H_2O per molecule. All non-hydrogen atoms except for some disordered crystal lattice toluene and CH_2Cl_2 were refined anisotropically. All hydrogen atoms in H_2bip and H_2bap except H7A and H15A in H_2bip were located directly from difference Fourier maps. Other hydrogen atoms were calculated, and their contributions were included. The crystallographic data, except for those of the free ligands and **3**·1.5C_7H_8, are given in Table 1. The data for the free ligands and **3**·1.5C_7H_8 are provided in the Supporting Information. Selected bond lengths and angles for the complexes are given in Table 2.

Quantum Yield Measurements. Emission quantum yields of complexes **1** and **2** were determined relative to 9,10-diphenylanthracene in THF at 298 K (Θ_r = 0.95).[13] The absorbances of all samples and the standard at the excitation wavelength were approximately 0.096−0.104. The quantum yields were calculated using previously reported procedures.[14] The excitation wavelength used for all samples is 400 nm.

Scheme 1

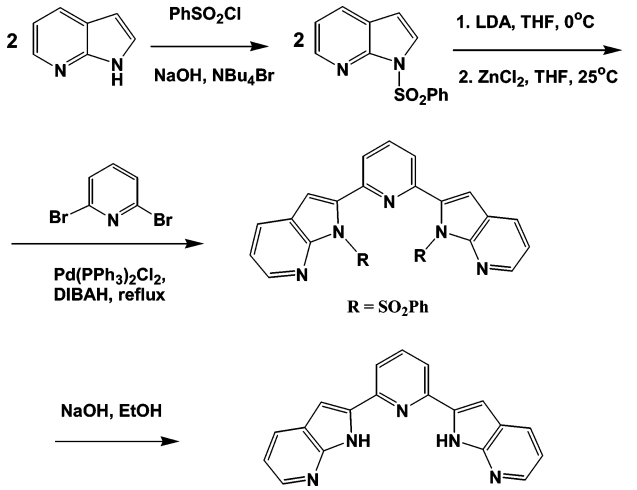

Results and Discussion

Ligands. The free ligand H_2bip was prepared in good yield by a two-step Fischer synthesis involving the coupling of 2,6-diacetylpyridine with 2 equiv of phenylhydrazine, according to previously reported methods.[9,10] However, using the same procedure to synthesize H_2bap by the coupling reaction of 2,6-diacetylpyridine with 2 equiv of 2-pyridylhydrazine was unsuccessful. The extra electronegative nitrogen atom in the 2-pyridylhydrazine molecule appears to have a dramatic effect on its reactivity in the Fischer cyclization reaction. The H_2bap ligand was synthesized by using a modified literature procedure, as shown in Scheme 1.[15] The NH site on the 7-azaindole molecule was first protected by a phenylsulfonyl group. The required [2-(7-azaindolyl)]-zinc chloride was easily obtained by metalation of 1-(phenylsulfonyl)-7-azaindole with LDA followed by the treatment of the resulting 2-lithium-7-azaindole with anhydrous $ZnCl_2$. Cross-coupling reactions of [2-(7-azaindolyl)]zinc chloride with 2,6-dibromopyridine in the presence of 2 mol % of a catalyst prepared from $PdCl_2$-$(PPh_3)_2$ and DIBAH (DIBAH = diisobutylaluminum hydride) in refluxing THF and the subsequent removal of the protecting group SO_2Ph afforded the H_2bap ligand in good yield. To study the impact of the coordination to a metal ion on the structure of the ligand, we examined the structures of H_2bip and H_2bap by single-crystal X-ray diffraction experiments.

The molecular structures of the free ligands are shown in Figure 1. Each molecule of H_2bip cocrystallized with one H_2O molecule, which forms two weak hydrogen bonds with the NH groups of the H_2bip ligand (Figure 1, top), as indicated by the O···N distances (3.006(5) and 3.028(5) Å, respectively). The mean deviation of atoms from the molecular plane is 0.047 Å, indicating that the pyridine ring and the two indolyl rings are coplanar. However, for H_2bap, the pyridine ring is not coplanar with the two 7-azaindolyl rings, and the dihedral angles between the 7-azaindolyl ring and the pyridine ring are 15.1 and 27.1°, respectively. This difference can be

(13) Murov, S. L.; Carmichael, I.; Hug, G. L. *Handbook of Photochemistry*, 2nd ed.; Marcel Dekker: New York, 1993.
(14) Demas, N. J.; Crosby, G. A. *J. Am. Chem. Soc.* **1970**, *92*, 7262.
(15) Liu, S. F.; Wu, Q.; Schmider, H. L.; Aziz, H.; Hu, N.-X.; Popovic, Z.; Wang, S. *J. Am. Chem. Soc.* **2000**, *122*, 3671.

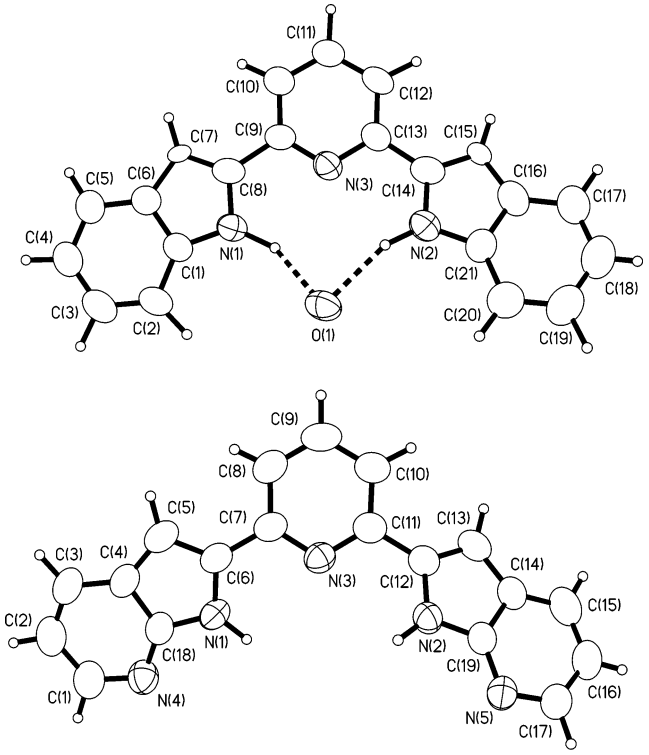

Figure 1. Molecular structures of H_2bip (top) and H_2bap (bottom) with 50% thermal ellipsoids and labeling schemes.

attributed to the presence of the hydrogen bonds in both molecules. For H_2bip, the chelation to the two indolyl rings by the H_2O molecule through hydrogen bonds clearly favors the coplanarity of the H_2bip ligand. For H_2bap, intermolecular hydrogen bonds between H_2bap molecules are believed to be responsible for its nonplanar structure. Although the molecular structures of H_2bip and H_2bap resemble each other, the extended structures of these two compounds in the crystal lattice are quite different. There is no interligand hydrogen bond present in the crystal of H_2bip due to the lack of accessible hydrogen acceptor sites. (The N(3) site is blocked, and the same is true for H_2bap.) In contrast, for H_2bap, N(1) and N(2) are hydrogen donors, while N(4) and N(5) atoms are hydrogen acceptors. Consequently, in the crystal lattice, the N(1) atom is paired with N(4A) of one neighboring molecule, while the N(2) atom is paired with N(5B) of the second neighboring molecule through hydrogen bonds, as evidenced by the distances of N(1)···N(4A) (2.950(4) Å) and N(2)···N(5B) (2.899(4) Å). The molecules of H_2bap couple through hydrogen bonds a manner that leads to the formation of an unusual *double-strand* structure, as shown in Figure 2. In addition to hydrogen bonds, *shape matching* between the H_2bap molecules also plays a role in the formation of the double-strand structure. As shown by Figure 2, there is a perfect shape match between each pair of molecules in the double strands. Clearly in order to maximize intermolecular hydrogen-bonding interactions, the two 7-azaindolyl rings must be out of plane with the pyridyl ring to minimizing nonbonding interactions, thus causing the nonplanarity of the molecule.

Complexes. As shown in Chart 1, to complete the coordination sphere of the Pt(II) center, a neutral ancillary ligand L is required to form the neutral complex Pt(bip)L. In the case of Sn(IV) and Pb(IV)

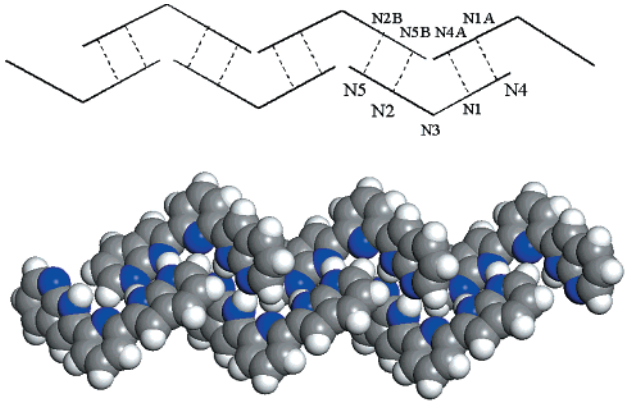

Figure 2. Hydrogen-bonded double-strand structure of H_2-bap: (top) diagram showing the hydrogen bond links; (bottom) space-filling diagram showing the hydrogen-bonded double strands. The gray atoms denote nitrogen and the white atoms hydrogen.

Scheme 2

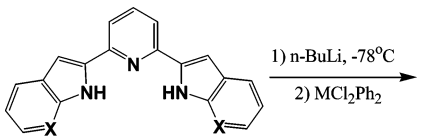

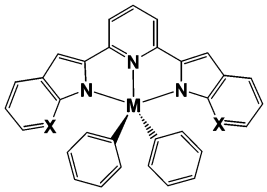

M = Sn, X = CH, (**1**)
M = Sn, X = N, (**2**)
M = Pb, X = CH, (**3**)
M = Pb, X = N, (**4**)

complexes, two 1− charged ligands are needed to saturate the coordination sphere of the metal center and to provide a neutral complex of M(bip)L_2 or M(bap)L_2. For this purpose, we chose MCl_2Ph_2 (M = Sn, Pb) as our starting materials. Although our attempts to synthesize Pt(bap)L have not been successful, the bap ligand was found, however, to be able to bind to Sn(IV) and Pb(IV) centers in the same manner as the bip ligand.

Complexes **1**−**4** were synthesized in good yield by substitution reactions where MCl_2Ph_2 (M = Sn, Pb) was reacted with the corresponding salt Li_2L (L = bip, bap) in a 1/1 ratio. The dilithium salts Li_2L were prepared from the reaction of n-BuLi and H_2L. The 2− charged ligand (bip or bap) replaced the Cl^- ions and tridentately chelated to the metal center, forming cyclometalated complexes with LiCl as byproduct. The syntheses of complexes **1**−**4** are summarized in Scheme 2. All complexes have been fully characterized by ^1H and ^{13}C NMR and elemental analyses. The ^{119}Sn NMR spectra were also recorded for complexes **1** and **2**, which display ^{119}Sn chemical shifts at −299.6 and −289.2 ppm (relative to $SnMe_4$), respectively, consistent with previously reported values for five-coordinated organotin(IV) complexes.[16] Attempts were made to record ^{207}Pb NMR spectra for complexes **3** and **4**. However, due to the poor solubility of compounds **3** and **4**, the ^{207}Pb chemical shifts for both complexes could not be located. Com-

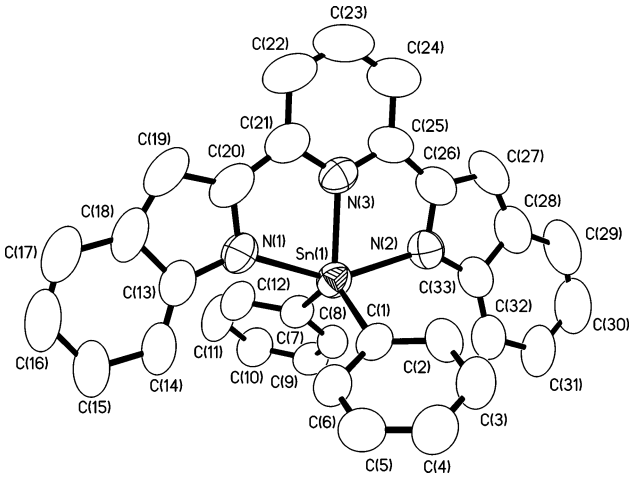

Figure 3. Molecular structure of complex **1** with 50% thermal ellipsoids and labeling schemes.

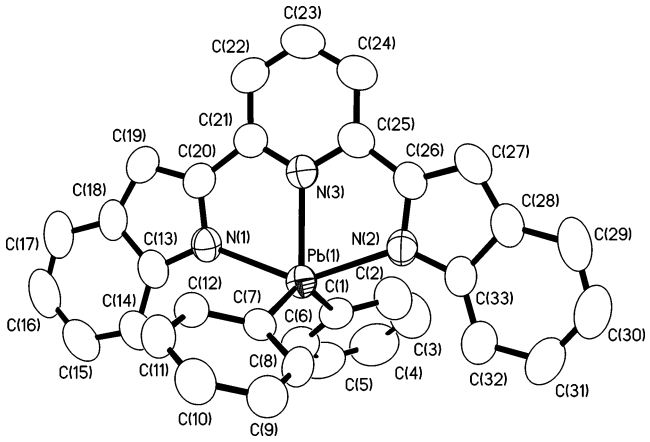

Figure 4. Molecular structure of complex **3** with 50% thermal ellipsoids and labeling schemes.

plexes **1**−**4** are stable under air in the solid state. The Sn(IV) complexes **1** and **2** are also stable in solution upon exposure to air. The Pb(IV) complexes **3** and **4**, in contrast, undergo slow decomposition in solution upon exposure to air. We also attempted the syntheses of Si(bip)Ph_2 and Si(bap)Ph_2 using the same procedure. However, these complexes are thermally unstable and undergo rapid decomposition upon isolation at ambient temperature. As a result, complete characterization for these two Si(IV) compounds could not be achieved. Although a number of organotin(IV) complexes involving cyclometalated ligands have been known previously, well-characterized organolead(IV) complexes containing cyclometalated ligands are scarce.[17,18] To fully establish the structures of the new Sn(IV) and Pb(IV) complexes, we carried out single-crystal X-ray diffraction analyses for all four complexes.

Crystal Structures. Complexes **1** and **2** have very similar molecular structures. The molecular structure of complex **1** is shown in Figure 3. In complexes **1** and **2**, the Sn(IV) center is five-coordinated. Each metal center is tridentately chelated by a bip or bap ligand via the N(1), N(2), and N(3) atoms in the same manner as in Pt(bip)L complexes.[9] In addition, two phenyl groups are coordinated to the metal center, forming a distorted-trigonal-bipyramidal geometry, as indicated by the N(1)−Sn(1)−N(2) angles of 148.19(19)° for **1** and 145.9(2)° for **2**, respectively, which are all much smaller than the ideal bond angle of an sp^3d hybrid orbital (180°). The bip and bap ligands in **1** and **2** are planar and coplanar with the Sn(IV) center, as indicated by the mean deviation of the Sn(1)N(1)N(2)N(3) plane being 0.005 Å for **1** and 0.015 Å for **2**, respectively. Clearly the chelation of the Sn(IV) ion to the bip and bap ligands reinforces the planarity of the ligands. The two phenyl groups are located above and below the bip or bap plane, respectively. The Sn−C bond lengths are in the typical range.[17,18d] However, the Sn−N bond lengths (average 2.177(5) Å) in both compounds are substantially shorter than most previously reported Sn−N bond lengths.[17a−d] The Sn−N bond lengths in **1** and **2** are close to those observed in $[Sn(tmtaa)Me]^+$ and $\{[Sn(tmtaa)]_2(CH_2)\}^{2+}$, where tmtaa is the macrocyclic ligand tetramethyltetraazadibenzo[14]annulene dianion.[17e,f] The closest intermolecular Sn···Sn distances are 7.360(5) Å for **1** and 7.527(7) Å for **2**, respectively.

The molecular structures of complexes **3** and **4** are similar and resemble those of complexes **1** and **2**. In the asymmetric units of complexes **3** and **4**, there are two independent molecules that display essentially the same structure. Complex **3** has two kinds of crystals with the same molecular structure but different crystal lattice solvents (CH_2Cl_2 and toluene, respectively). The discussion here focuses on the CH_2Cl_2-solvated structure. One of the independent molecules of **3**·CH_2Cl_2 is shown in Figure 4. The Pb(IV) centers in **3** and **4** are five-coordinate with a distorted-trigonal-bipyramidal geometry. However, the degree of distortion by **3** and **4** is more than that of **1** and **2**, as indicated by the C(1)−Pb(1)−C(7) angle (138.19(15) and 154.2(4)° for **3** and **4**, respectively) and the N(1)−Pb(1)−N(2) angle (141.59(12) and 138.0(5)° for **3** and **4**, respectively), which is attributable to the relatively large size of the Pb(IV) ion. Similar distorted-trigonal-bipyramidal structures have been observed previously for organolead(IV) compounds.[18] The Pb−C and Pb−N bond lengths in **3** and **4** are about 0.1 Å longer than the corresponding Sn−C and Sn−N bonds in **1** and **2**. The Pb−C bond lengths of **3** and **4** are similar to those in previously reported organolead(IV) compounds.[18] The Pb−N bond lengths displayed by **3** and **4** are, however, among the shortest, compared to Pb−N distances in previously known Pb(IV) compounds.[18] Similar to the case for **1** and **2**, the Pb centers in **3** and **4** are also coplanar with the planes of bip or bap ligands. The shortest intermolecular Pb···Pb distances in **3**·CH_2Cl_2 and **3**·1.5C_7H_8 are 7.780(4) and 6.755(6) Å, respectively.

(16) Davis, A. G. In *Comprehensive Organometallic Chemistry*; Wilkinson, G., Stone, F. G. A., Abel, E. W., Ed.; Pergamon Press: Oxford, U.K., 1982; Vol. 2, Chapter 11, p 519.

(17) (a) van Koten, G.; Jastrzebski, J. T. B. H.; Noltes, J. G.; Pontenagel, W. M. G. F.; Kroon, J.; Spek, A. J. *J. Am. Chem. Soc.* **1978**, *100*, 5021. (b) van Koten, G.; Noltes, J. G. *J. Organomet. Chem.* **1976**, *118*, 183. (c) García-Zarracino, R.; Ramos-Quiñones, J.; Höpfl, H. *J. Organomet. Chem.* **2002**, *664*, 188. (d) van Koten, G.; Jastrzebski, J. T. B. H.; Noltes, J. G.; Verhoeckx, G. J.; Spek, A. L.; Kroon, J. *J. Chem. Soc., Dalton Trans.* **1980**, 1352. (e) Belcher, W. J.; Brothers, P. J.; Meredith, A. P.; Richard, C. E. F.; Ware, D. C. *J. Chem. Soc., Dalton Trans.* **1999**, 2833. (f) Belcher, W. J.; Brothers, P. J.; Land, M. V.; Richard, C. E. F.; Ware, D. C. *J. Chem. Soc., Dalton Trans.* **1993**, 2101.

(18) (a) Yatsenko, A. V.; Aslanov, A. *Polyhedron* **1995**, *14*, 2371 and references therein. (b) Harrison, P. G. In *Comprehensive Organometallic Chemistry*; Wilkinson, G., Stone, F. G. A., Abel, E. W., Eds.; Pergamon Press: Oxford, U.K., 1982; Vol. 2, Chapter 12, p 629. (c) Yatsenko, A. V.; Schlenk, H.; Aslanov, L. A. *J. Organomet. Chem.* **1994**, *474*, 107. (d) Onyszchuk, M.; Wharf, I. *J. Organomet. Chem.* **1987**, *326*, 25.

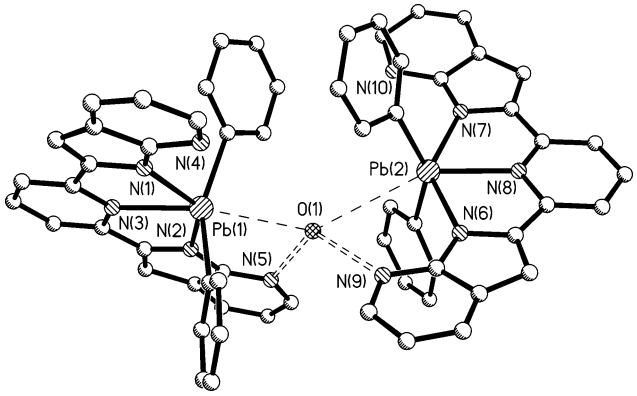

Figure 5. Hydrogen-bonded dimer structure of complex **4** with labeling schemes.

Table 3. UV−Vis Data for H_2Bip, H_2Bap, Pt(bip)(SMe_2), Pt(bip)Py, and 1−4

compd	absorption (nm) (ϵ, $M^{-1}\,cm^{-1}$) in THF, 298 K[a]
H_2bip	322 (27 900), 354 (33 400), 418 (77)
H_2bap	322 (23 450), 350 (26 340), 418 (194)
Pt(bip)SMe_2	336 (37 260), 350 (38 780), 426 (30 600)
Pt(bip)Py	350 (27 400), 418 (21 800)
1	336 (9700), 430 (7560)
2	340 (8300), 422 (7700)
3	330 (17 660), 426 (20 020)
4	338 (13 470), 412 (14 830)

[a] [M] = (1.3×10^{-5})−(2.2×10^{-5}) M.

In the asymmetric unit of the crystal of **4** are two independent molecules that are coupled together through a H_2O molecule via hydrogen bonds between the H_2O molecule and two noncoordinating nitrogen atoms (N(5) and N(9)) of two 7-azainolyl groups, forming a dimer structure (Figure 5). The distances of O(1)···N(5) and O(1)···N(9) are 2.681(13) and 2.745(12) Å, respectively. The distance between the two Pb(IV) centers is 6.077-(12) Å. The Pb(1)···O(1) and Pb(2)···O(1) distances are 2.981(8) and 3.448(8) Å, respectively, slightly shorter than the sum of van der Waals radii of Pb and O (3.54 Å) but much longer than the sum of covalent radii (∼2.20 Å), suggesting the presence of very weak interactions between the water O(1) atom and the two Pb-(IV) centers.

Another interesting feature of complexes **1**, **2**, **3**·CH_2-Cl_2, and **4** is that they all form similar 1D $\pi-\pi$ stacking columns in the solid state involving the back-to-back stacking of bip or bap ligands of adjacent molecules. Two representative $\pi-\pi$ stacking columns from the crystal lattices of **1** and **3**·CH_2Cl_2 are shown in Figure 6 (top and middle diagrams). All the columns are parallel to each other in the crystals of **1**−**4**, and between these columns are trapped solvent molecules, CH_2Cl_2 or toluene (see unit cell packing diagrams in the Supporting Information). The distances between the $\pi-\pi$ stacked aromatic planes in these crystals range from 3.43 to 3.71 Å. For compound **4**, the 1D $\pi-\pi$ stacking columns are similar to those of **1**−**3**·CH_2Cl_2, except that these 1D columns are linked together by H_2O molecules via hydrogen bonds as depicted in Figures 5 and 6 (bottom diagram). In the crystal of complex **3**·1.5C_7H_8, only one of the independent molecules is involved with $\pi-\pi$ stacking, and it does not form the 1D column structure similar to **1** and **2**. Instead, it forms a $\pi-\pi$ stacking dimer structure (see the Supporting Information). The

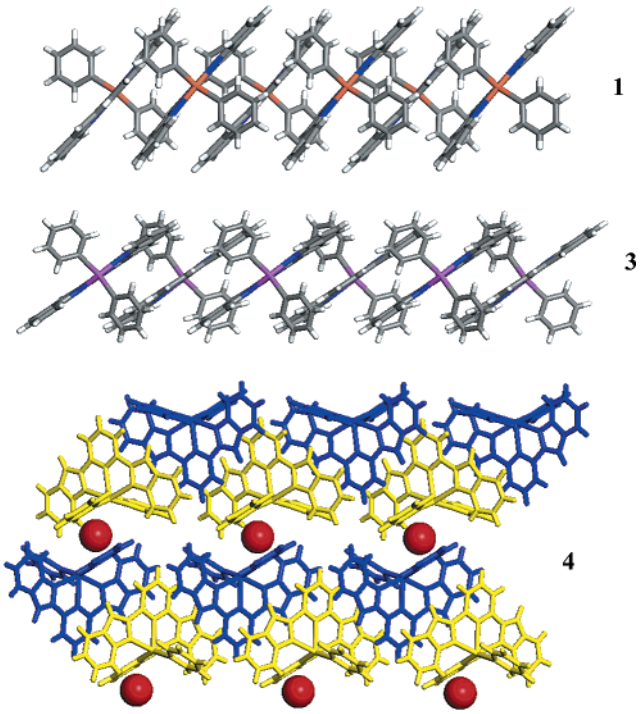

Figure 6. Diagrams showing (top) the 1D back-to-back $\pi-\pi$ stacking column of **1**, (middle) the 1D back-to-back $\pi-\pi$ stacking column of **3** (solvated by CH_2Cl_2), and (bottom) the 1D back-to-back $\pi-\pi$ stacking column of **4** and the location of H_2O molecules that link two molecules of **4** through hydrogen bonds. This last view is rotated by ∼90° from a view similar to that in the middle diagram. H_2O molecules are shown as red balls.

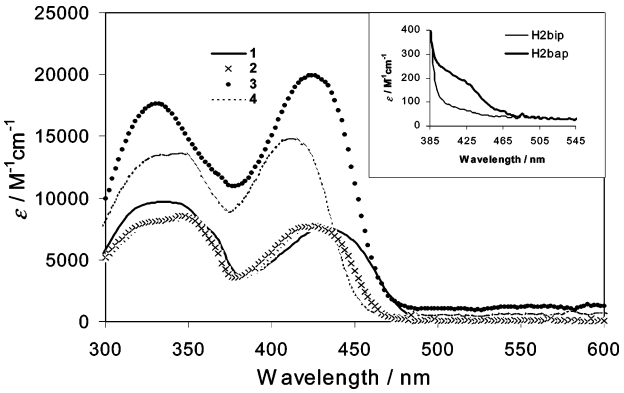

Figure 7. UV−vis spectra of complexes **1**−**4** in THF solution. Inset: UV−vis spectra of H_2bip and H_2bap in the 400−550 nm region.

distance between the two stacking planes of the bip ligands in **3**·1.5C_7H_8 is 3.49 Å.

UV−Vis Absorption Spectra. Complexes **1**−**4** display very similar absorption bands. As shown in Figure 7, these four complexes have two main absorption bands, one with $\lambda_{max} \approx 330-340$ nm and the other at 412−430 nm, both of which resemble those of the Pt-(bip)L complexes we reported previously (Table 3),[9] an indication that these absorption bands are likely due to ligand-centered transitions. The free H_2bip and H_2-bap ligands display a similar intense absorption band with $\lambda_{max} \approx 330-340$ nm. Therefore, the absorption band of the complexes with $\lambda_{max} \approx 330-340$ nm is attributed to the spin-allowed singlet $\pi \rightarrow \pi^*$ transition. Because the free ligands H_2bip and H_2bap have a very

weak absorption band (ϵ = 81 and 194 M^{-1} cm^{-1}, respectively) at $\lambda_{max} \approx$ 418 nm (Figure 7, inset), we assigned the absorption bands of the complexes at $\lambda_{max} \approx$ 412−430 nm to the spin-forbidden triplet $\pi \rightarrow \pi^*$ transition. The fact that the extinction coefficients of the complexes for the absorption bands at 412−430 nm are much greater than those of the corresponding free ligand (Table 3) led us to believe that the Sn(IV) and the Pb(IV) centers greatly enhance the triplet electronic transition of the ligands. This is consistent with the well-established phenomena that heavy-metal atoms can play a key role in promoting singlet−triplet mixing, hence enhancing triplet transitions.[4] Furthermore, the extinction coefficients of the Pb(IV) complexes **3** and **4** are about 2−3 times greater than those of the Sn(IV) complexes **1** and **2** (Figure 7 and Table 3), consistent with the fact that the Pb atom is heavier than Sn and, hence, more efficient in promoting triplet electronic transitions.

Luminescent Properties. We have reported that the neutral H_2bip ligand is a bright blue emitter with an emission maximum at λ = 401 nm in solution and at λ = 430 nm in the solid state at ambient temperature.[9] Similarly, the neutral H_2bap ligand has been found to be a bright blue emitter in solution with an emission maximum at λ = 397 nm. However, in the solid state, H_2bap exhibits a bright greenish blue color with an emission maximum at λ = 477 nm, red-shifted about 80 nm from its emission in solution. This dramatic red shift is attributed to intermolecular interactions of H_2-bap in the solid state, most likely the hydrogen-bond-linked double-strand polymer structure as shown in Figure 2. At 77 K in a frozen THF solution, H_2bap displays an intense fluorescent emission band at 394 nm. Using a time-resolved phosphorescence spectrometer, a weak phosphorescent emission band at 558 nm with a shoulder at 597 nm was also observed. The decay lifetimes for the phosphorescent emission bands were determined to be 74.5(5) and 96.6(6) μs, respectively. Similar phosphorescent emission (λ_{max} = 571 nm, τ = 63.9(2) μs) was also observed for H_2bip at 77 K.[9]

At ambient temperature, in solution, the Sn(IV) complexes **1** and **2** display intense emission bands at 515 and 490 nm, respectively, and the quantum yields were determined to be 0.087 for **1** and 0.19 for **2**. These emission bands are dominated by fluorescence. In the solid state at ambient temperature, the emissions are red-shifted to 534 nm for **1** and 500 nm for **2,** respectively, due to intermolecular interactions—most likely intermolecular $\pi-\pi$ stacking interactions, as demonstrated by single-crystal X-ray diffraction analyses (Figure 6). In contrast, the Pb(IV) complexes **3** and **4** are not luminescent either in solution or in the solid state at ambient temperature, which is not surprising, since Pb is much heavier than Sn, hence leading to a more efficient fluorescence quenching[19] compared to Sn. At 77 K, the THF solutions of all four complexes display intense luminescence. For the Sn(IV) complexes **1** and **2**, the 77 K emission was dominated by fluorescence

(19) (a) Drago, R. S. *Physical Methods in Chemistry*, W. B. Saunders: Philadelphia, PA, 1977; Chapter 5. (b) Masetti, F.; Mazzucato, U.; Galiazzo, G. *J. Lumin.* **1971**, *4*, 8. (c) Werner, T. C.; Hawkins, W.; Facci, J.; Torrisi, R.; Trembath, T. *J. Phys. Chem.* **1978**, *82*, 298. (d) Bluemer, G. P.; Zander, M.; Ruetgerswerke, A. G. *Z. Naturforsch., A* **1979**, *34A*, 909.

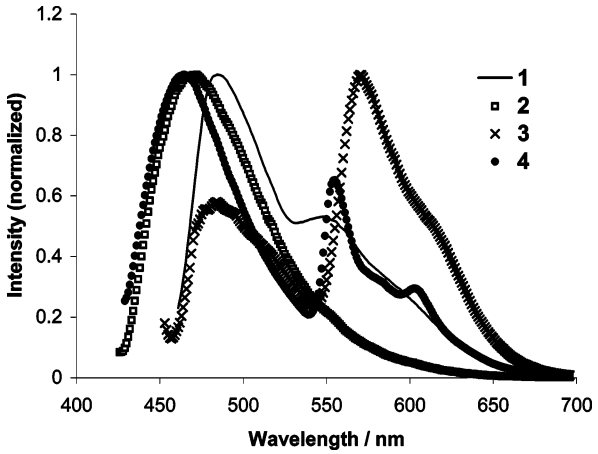

Figure 8. Full emission spectra of complex **1**−**4** at 77 K in THF.

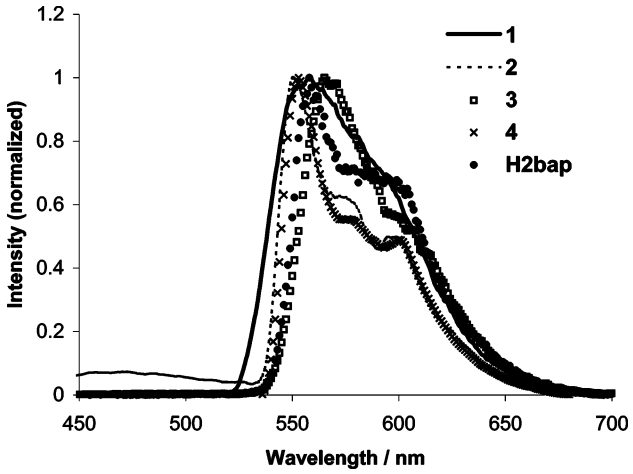

Figure 9. Phosphorescent emission spectra of complexes **1**−**4** and H_2bap in THF at 77 K obtained using a time-resolved phosphorescence spectrometer.

(λ_{max} = 485, 470 nm for **1** and **2**, respectively) with a shoulder phosphorescent band at ∼557 nm (Figure 8). For the Pb(IV) complexes **3** and **4** well-resolved fluorescent and phosphorescent emission bands were observed. The fluorescent bands of **3** and **4** are at λ_{max} = 489 and 465 nm, respectively, while the phosphorescent emission bands are at λ_{max} = 571, 555, and 603 nm (shoulder), respectively. In fact, for complex **3**, the 77 K emission in THF solution was dominated by the phosphorescent emission band with λ_{max} = 571 nm. Using a time-resolved phosphorescent spectrometer, we were able to completely remove the fluorescent emission band. The resulting phosphorescent emission bands for all complexes are shown in Figure 9, which is very similar to the phosphorescent emission bands of Pt(bip)L complexes reported previously.[9] The phosphorescent decay lifetimes of the complexes were found to range from 8.98(6) to 19.6(9) μs (Table 4), which are comparable with those of the Pt(bip)L complexes. The phosphorescent emissions of complexes **1** and **3** and of **2** and **4** are in the same region of the phosphorescent emission of the corresponding H_2bip or H_2bap ligand (Table 4). Therefore, we conclude that the phosphorescent emission of the complexes is ligand-based, involving most likely $\pi \rightarrow \pi^*$ transitions.

The striking difference between the free ligands and the complexes is that the phosphorescent emissions of

Table 4. Fluorescence and Phosphorescence Data for Compounds 1−4

compd	λ_{max}, nm excitation	λ_{max}, nm emission	decay lifetime (τ, μs)[a]	conditions
1	466	515		THF, 298 K
	466	534		solid, 298 K
	448	485		THF, 77 K
		557 (sh)[b]	14.6(5)	THF, 77 K[c]
2	455	490		THF, 298 K
	466	500		solid, 298 K
	410	470		THF, 77 K
	422	551	10.9(3)	THF, 77 K[c]
		597	8.98(6)	
3	437	489	0.22(1) ns, 6.67(1) ns	THF, 77 K
		571	19.6(9)	THF, 77 K[c]
4	416	465		THF, 77 K
		555	17.6(6)	THF, 77 K[c]
		603 (sh)	15.6(6)	

[a] A reliable lifetime could not be obtained for the fluorescent emission due to the limitation of our spectrometer. The fluorescent decay lifetime for **3** was measured by Photon Technology International (Canada) Inc. [b] sh = shoulder. [c] Obtained using a time-resolved phosphorescence spectrometer.

the complexes are much brighter and the decay lifetimes (10−20 μs) are much shorter than those of the free ligands (60−100 μs) and, hence, are much more easily detectable. Clearly, as the Pt(II) centers in Pt(bip)L complexes,[9] the Sn(IV) and Pb(IV) centers in complexes **1**−**4** play a key role in enhancing the phosphorescent emission of the ligands. The chelation of the bip or bap ligands to the metal center also contributes to the enhancement of the phosphorescent emission by increasing the rigidity of the ligands, thus reducing the loss of energy by thermal vibrational decay.[6] From Figure 8, it is evident that the phosphorescent emissions of **3** and **4** are much more intense than those of **1** and **2**, again supporting the notion that the Pb(IV) center is much more efficient in enhancing phosphorescent emission than Sn(IV), consistent with the fact that the Pb(IV) center is more efficient in promoting triplet electronic transitions, as demonstrated by the UV−vis spectral data.

In comparison to the emission spectra of Pt(bip)L complexes, where the fluorescent emission band of the bip ligand vanishes completely,[9] the Sn(IV) and Pb(IV) centers in complexes **1**−**4** only partially diminish the intensity of the fluorescent emission of the ligands, relative to that of the phosphorescent emission. The fact that the fluorescent emission band of the bip or bap ligands is well-resolved and fairly intense in the complexes **1**−**4** (Figure 7) led us to suggest that the Sn(IV) and Pb(IV) centers appears to be not as effective as the Pt(II) center in promoting $^1S \rightarrow {}^3T$ intersystem crossing and, hence, phosphorescence of the bip or bap ligand, the cause of which is yet to be understood.

In summary, new five-coordinated organotin(IV) and organolead(IV) complexes based on H_2bip and H_2bap ligands have been synthesized. These complexes display both blue-green fluorescent and orange-red phosphorescent emissions that involve ligand-centered $\pi \rightarrow \pi^*$ transitions. The role of the group 14 elements Pb(IV) and Sn(IV) in enhancing phosphorescent emission of the ligand has been demonstrated. The relatively short decay lifetime of the phosphorescent emissions and the chemical stability in the solid state make these complexes potentially useful as emitters for OLEDs. However, the presence of fluorescent emission of the new complexes is a concern to us with regard to the effectiveness of these complexes as phosphorescent emitters in OLEDs. Efforts to evaluate the actual performance of these new complexes in OLEDs are being undertaken.

Acknowledgment. We thank the Natural Sciences and Engineering Research Council of Canada for financial support.

Supporting Information Available: X-ray diffraction data for H_2bip, H_2bap, and complexes **1**−**4**, including tables of atomic coordinates, thermal parameters, bond lengths and angles, and hydrogen parameters and unit cell packing diagrams, and figures giving room-temperature emission spectra of **1** and **2**. This material is available free of charge via the Internet at http://pubs.acs.org.

OM030404A